Atmospheric Measurement Techniques
Open Access
Discussions

Mobile measurements of ship emissions in two harbour areas in Finland

L. Pirjola[1,2], A. Pajunoja[3,4], J. Walden[5], J.-P. Jalkanen[5], T. Rönkkö[3], A. Kousa[6], and T. Koskentalo[6]

[1]Department of Technology, Metropolia University of Applied Sciences, Helsinki, Finland
[2]Department of Physics, University of Helsinki, Helsinki, Finland
[3]Aerosol Physics Laboratory, Department of Physics, Tampere University of Technology, Tampere, Finland
[4]Department of Applied Physics, University of Eastern Finland, Kuopio, Finland
[5]Air Quality, Finnish Meteorological Institute, Helsinki, Finland
[6]Helsinki Region Environmental Services Authority HSY, Helsinki, Finland

Title Page

Abstract	Introduction
Conclusions	References
Tables	Figures

|◄ | ►|
◄ | ►
Back | Close

Full Screen / Esc

Printer-friendly Version

Interactive Discussion

Abstract

Four measurement campaigns by a mobile laboratory van were performed in two different environments; inside the harbour areas in the city center of Helsinki and along the narrow shipping channel near the city of Turku, Finland, during the winter and summer conditions in 2010–2011. The characteristics of gaseous (CO, CO_2, SO_2, NO, NO_2, NO_x) and particulate (number and volume size distributions as well as $PM_{2.5}$) emissions for 11 ships regularly operating on the Baltic Sea were studied to determine the emission parameters. The highest particle concentrations were 1.5×10^6 and 1.6×10^5 cm^{-3} in Helsinki and Turku, respectively, and the particle number size distributions had two modes. The dominating mode was peaking at 20–30 nm and the accumulation mode at 80–100 nm. The majority of the particle mass was volatile since after heating the sample to 265 °C, the particle volume of the studied ships decreased by around 70 %. The emission factors for NO_x varied in the range of 25–100 g (kg fuel)$^{-1}$, for SO_2 in the range of 2.5–17.0 g (kg fuel)$^{-1}$, for particle number in the range of (0.32–2.26) × 10^{16} particles (kg fuel)$^{-1}$, and for $PM_{2.5}$ between 1.0–4.9 g (kg fuel)$^{-1}$. The ships equipped with SCR had lowest NO_x emissions whereas the ships with DWI and HAM had lowest SO_2 emissions but highest particulate emissions. For all ships the averaged fuel sulphur contents (FSCs) were less than 1 % (by mass) but none of those was below 0.1 % which will be the new EU directive from 1 January 2015 in the SO_x Emission Control Areas, indicating big challenges for ships operating on the Baltic Sea.

1   Introduction

More than 80 % of world trade is transported by ships (Fuglestvedt et al., 2009). Large ships are primarily powered by diesel propulsion systems and usually fuelled by heavy fuel oil (HFO). HFO is low-grade fuel that includes high concentration of impurities such as sulphur, ash, asphaltenes, and metals (Sinha et al., 2003). Distillates are refined fuels, but due to their higher costs, they are generally used by small, medium

speed diesel engines such as auxiliary engines for port activities, and by main engines for manoeuvring in harbour areas (Saxe and Larsen, 2004). Marine traffic is a significant source of diesel emissions affecting global climate, air quality and human health. Emitted CO_2 and ozone formed by NO_x emissions are greenhouse gases whereas SO_2 emissions cause cooling through effects on atmospheric particles and clouds. The present net effect is cooling (Fuglestvedt et al., 2009). Around two third of ship emissions occurs within 400 km of coastlines leading to reduced air quality in coastal areas and harbours. Corbett et al. (2007) estimated that shipping-related $PM_{2.5}$ emissions are responsible for approximately 60 000 premature cardiopulmonary and lung cancer deaths annually at a global scale.

Shipping emits both primary and secondary particles. Incomplete combustion of carbon produces primary soot particles. Besides organic carbon, elemental carbon and ash, these particles also include vanadium, nickel and sulphur due to impurities in HFO. Fuel sulphur is oxidized to SO_2 and further to SO_3 during combustion. The amount of SO_3 depends on the combustion temperature, but the reaction is catalyzed by the presence of vanadium (Isakson et al., 2001). During dilution and cooling SO_3 reacts with water vapour forming sulphuric acid which subsequently can nucleate to form secondary particles and/or condense onto pre-existing particles (Arnold et al., 2006). Nanoparticle emissions depend on the technology parameters; fuel, after-treatment system used, and operating conditions e.g. engine load, ship's speed and acceleration. Eyring et al. (2005) and Fridell et al. (2008) have reported that a selective catalytic reduction (SCR) is able to significantly reduce the emissions of marine diesel engine; for example, particle mass emissions by 50 % over the whole size range, and for full load the mass emissions of NO_x by 90–99 %, HC and CO by 80–90 %, and soot by 30–50 %. Different scrubbing systems have been commonly applied to diesel power plants on land, but until now their commercial installation on ships have been scarce (Jalkanen et al., 2012). Still many ship engines operate without any after-treatment systems.

Mobile measurements of ship emissions

L. Pirjola et al.

Most of the literature studies focus on NO_x, SO_x, and PM emissions. Recent publications have started to be concerned with nanoparticle emissions and their measurement (see a recent review paper by Kumar et al., 2013). The studies have been performed in laboratory conditions on engine test beds (Kasper et al., 2007; Lyyränen et al., 1999; Petzold et al., 2008), on-board from the ship pipe (Agrawal et al., 2008b; Fridell et al., 2008; Moldanova et al., 2009; Murphy et al., 2009), in ship plumes by aircraft (Murphy et al., 2009; Petzold et al., 2008; Sinha et al., 2003) or by ships (Lack et al., 2009), as well as by performing stationary measurements in the port areas (Ault et al., 2009; Healy et al., 2009; Isakson et al., 2001; Jonsson et al., 2011). The number emission factors are in the range of $(1.3–6.2) \times 10^{16}$ particles per kg fuel burnt. Typically, a bimodal number size distribution was found; the nucleation mode peaking at $< 20\,nm$ and the Aitken mode at $50–100\,nm$.

Ship emissions are one of the least regulated sources of anthropogenic emissions (Eyring et al., 2005). The International Maritime Organization (IMO) which is responsible for the international regulations of pollutants from ships has set the emission limits for NO_x and SO_x in the revised Marpol Annex VI rules (IMO, 1998). National or regional regulations call for even more stringent limits than those given by the IMO. For example, in June 2004, the EU environment ministers agreed a 1.5 % sulphur (by mass) limit for fuels used by all ships in the Baltic Sea, North Sea and English Channel (Eyring et al., 2005), and currently use of 0.1 % sulphur by seagoing ships at berth is required in EU ports (European Union, 2012). Additionally, because the Baltic Sea is an emission control area for SO_x (SECA) the ships operating there must use reduced–sulphur fuels (fuel sulphur content less than or equal to 1 % by mass) from 1 July 2010, and this will be decreased to 0.1 % in January 2015. The Baltic Sea is a busy area for short–sea marine traffic; about 3500–5000 different vessels are in operation every month (Jalkanen et al., 2012).

This study is a part of the SNOOP (Shipping-induced NO_x and SO_x emissions – Operational monitoring network) project which aims to find out how ship exhaust emissions are effecting to marine environment and human health in harbour areas. The

Mobile measurements of ship emissions

L. Pirjola et al.

more detailed objectives of this work were to measure and characterise the emissions of regular operating ships equipped with different after-treatment systems under winter and summer conditions in two different environments in Finland.

2 Experimental methods

2.1 Measurement sites

The measurements of ship emissions by a mobile laboratory van called "Sniffer" (see Sect. 2.2) were performed in two different harbour environments in Finland; at the harbours in the Helsinki downtown area, and along the shipping channel in a city of Turku (Fig. 1). The wintertime campaigns were conducted in Helsinki on 18–29 January 2010 and 7 January–25 February 2011, and in Turku 2–28 February 2010 and 7–17 February 2011. The summertime campaigns were performed on 26 July–6 August 2010 and 25 July–15 September 2011 in Helsinki, and 9–19 August 2010 and 1–10 August 2011 in Turku. Monitoring occurred in the morning at 07:00–12:00 and in the evening at 16:00–22:00, all times are local times. During the winter campaigns the mean temperature was $-4.6 \pm 5.8\,^\circ$C in Helsinki and $-4.7 \pm 4.3\,^\circ$C in Turku. As typical for Finnish winters the variation was very high. The mean relative humidity was $83 \pm 6\,\%$ for both locations. During the summer campaigns the temperature variation was lower, and the mean temperatures were $20 \pm 3\,^\circ$C and $19 \pm 1\,^\circ$C for Helsinki and Turku, respectively, whereas the mean relative humidity varied highly between 40–90 % the mean values being $73 \pm 8\,\%$ in Helsinki and $66 \pm 11\,\%$ in Turku.

Passenger traffic is busy at South Harbour of Helsinki. The Viking Line ships daily operate between Helsinki–Stockholm and Helsinki–Tallinn from the Katajanokka terminal (sites 1 and 2 in the right side panel in Fig. 1). The Tallink Silja Line ships daily operate from the Olympic terminal (site 4) between Helsinki–Stockholm and from the Makasiini terminal (site 3) to St. Petersburg and Tallinn. All of these ships are passenger ships but as well they provide roro service (ROPAX ships), and in fact, a lot of cars and trucks

are travelling with them. Additionally, during summer times many cruisers visit South Harbour (sites 1–4) and West Harbour (site 7). Pollutants from other local sources such as city traffic and a power plant located at 2 km distance from South Harbour affect air quality in the harbours as well. For example, the SO_2 concentrations measured in the harbour area are highest with south-eastern wind due to the ships and with northern wind due to the power plant (Fig. 2).

The measurement site was chosen according to the wind direction so that with south wind Sniffer was standing at sites 1 and 2, with east or north-easterly wind at sites 3–4, and with south wind in summer at site 7.

Furthermore, ships of Tallink Silja Line and Viking Line operate daily between Turku and Tukholma departing from Turku Harbour. The passenger and freight traffic regularly occurs in the mornings and evenings. Depending on the wind direction each measurement site (1–8 in the left side panel, Fig. 1) along the shipping channel was chosen so that the ship plume likely entered the sampling inlet of Sniffer. The distance of the measurement site from the ship line varied between 100 and 1000 m, and the measurement sites located within the distance of around 5 km from the harbour. Other local sources were minimal since no busy roads and only a few buildings were close to the sites. However, northern winds might transport pollution from the city center and harbour to the measurement sites (Fig. 3).

With south-westerly or north-easterly wind Sniffer was standing at sites 1 and 5, with eastern or western wind at site 2, and with southern or south-westerly wind at sites 3, 4, 7 and 8, even though site 4 was used with north-easterly wind as well.

2.2 Instrumentation for mobile measurements

Monitoring was conducted with a mobile laboratory van Sniffer (VW LT35 diesel van) described in detail in Pirjola et al. (2004, 2006, 2012). Sniffer was parked at the measurement site, heading to the ship plume. The sampling occurred at 2.4 m height from the ground level, above the van's windshield. All instruments were zero checked and synchronized before the start of the measurements.

Title Page

Abstract | Introduction

Conclusions | References

Tables | Figures

◄ | ►

Back | Close

Full Screen / Esc

Printer-friendly Version

Interactive Discussion

Particle number concentration and size distribution were measured with an ELPI (Electrical Low Pressure Impactor, Dekati Ltd.) (Keskinen et al., 1992) equipped with a filter stage (Marjamäki et al., 2002) and an additional stage designed to enhance the particle size resolution for nanoparticles (Yli-Ojanperä et al., 2010). In the ELPI, the particles with aerodynamic diameters in the size range of 7 nm–10 µm are first charged and then classified into 12 stages with a time resolution of 1 s. The cut-off diameters of the ELPI stages are 0.016 (additional stage), 0.030, 0.056, 0.093, 0.156, 0.264, 0.385, 0.617, 0.954, 1.610, 2.410, and 9.97 µm. In some measurements a thermodenuder TD (Rönkkö et al., 2011) was used to study particle volatility characteristics at the maximum operating temperature of 265 °C. For these cases, the ELPI measured the plume after the TD, and another ELPI (without the additional stage) was installed before the TD. The particle concentrations were corrected for particle losses in the TD.

A DustTrak (TSI, model 8530) with a 2.5 µm cut-off size was used to measure the real-time $PM_{2.5}$ concentration (i.e. particles less than 2.5 µm in aerodynamic diameter) with a time resolution of 1 s. The DustTrak operates based on a light scattering technique where the amount of the scattered light is proportional to the volume concentration of the aerosol. The instrument was factory calibrated with Arizona dust particles. Different correction factors for DustTraks under various environments have been published (e.g. Morawska et al., 2003; Wierzbicka, 2008). However, in this work the relative $PM_{2.5}$ values are enough for calculating the emission factors, and thus absolute $PM_{2.5}$ values are not needed.

Gaseous concentrations such as CO_2 (model VA 3100, Horiba), CO (model CO12M, Environnement S.A.), nitrogen oxides NO, NO_2 and NO_x (model APNA 360, Horiba), and SO_2 (Thermo Environmental Instruments, Model 43 C) were monitored above the windshield of Sniffer at the same altitude as particle concentrations with a time resolution of 1 s. A weather station on the roof of the van at a height of 2.9 m above the ground level provided meteorological parameters. Relative wind speed and direction were measured with an ultrasonic wind sensor (model WAS425AH, Vaisala); the temperature and relative humidity with temperature and humidity probes (model HMP45A,

Vaisala). Additionally, a global positioning system (model GPS V, Garmin) saved the van's speed and the driving route. Distance between a ship and Sniffer was continuously measured by a Newcon Optik–Laser Rangefinder Monocular (LRM2500) up to 2.285 km.

2.3 Ship characterization

In this work, the emissions of 11 ships were studied when they were normally operating. The main engines of all the ships were marine diesel engines which used HFO as fuel. Four of the ships were equipped by the SCR system (Selective Catalytic Reduction), one used HAM (Humid Air Motor) method, and two DWI (Direct Water Injection) method to decrease NO_x emissions (Table 1). Also given in Table 1 is the maximum power of the four main engines.

2.4 Emission parameters

Emission ratio ER_X is defined as a ratio of the excess concentration of X emitted from a source divided by the excess concentration of CO_2 emitted by the source

$$ER_X = \frac{X - X_{bg}}{CO_2 - CO_{2,bg}} = \frac{\Delta X}{\Delta CO_2} \tag{1}$$

where X is gaseous or particle number or mass concentration, and X_{bg} and $CO_{2,bg}$ are background concentrations. ER_X can as well be calculated directly from the regression slope of the concentration of ΔX to that of ΔCO_2 (Andreae and Merlet, 2001). If the instruments measuring X and CO_2 have about the same time response, the peak concentrations of X and CO_2 can be used to calculate ER and EF, otherwise the integrals have to be used (Schlager et al., 2007; Petzold et al., 2008). For comparison, we calculated the emission ratios and emission factors in this work in both ways.

Since in this work the gases (SO_2, NO, NO_2, NO_x, CO_2) were measured in ppm, number concentration in particles cm^{-3}, and PM concentration in $\mu g\,m^{-3}$, the units of

ER_X are $ppm\,ppm^{-1}$ for gases, $cm^{-3}\,ppm^{-1}$ for N_{tot}, and $\mu g\,m^{-3}\,(\mu g\,m^{-3})^{-1}$ for $PM_{2.5}$ if the CO_2 concentration is converted to mass unit by the ideal gas law at NTP conditions ($T = 293.15\,K$).

Emission factor EF_X ($g\,kg^{-1}$) is the amount of compound X released per amount of fuel burned and can be expressed as

$$EF_X = ER_X \cdot \frac{M_X}{M_{CO_2}} \cdot EF_{CO_2} \qquad \text{for gases} \qquad (2a)$$

$$EF_{N_{tot}} = ER_{N_{tot}} \frac{RT}{p \cdot M_{CO_2}} \cdot EF_{CO_2} \qquad \text{for particle number concentration} \qquad (2b)$$

$$EF_{PM_{2.5}} = ER_{PM_{2.5}} \cdot EF_{CO_2} \qquad \text{for particle mass concentration} \qquad (2c)$$

where M_X and M_{CO_2} are the mole masses of the gases X and CO_2, and EF_{CO_2} is the emission factor of the reference species CO_2. In this work we used a value of 3107 g per kg fuel burned (Petzold et al., 2008). Note that for particle number concentration, the unit of EF is particles per kg fuel burned.

2.5 Fuel sulphur content

If the emission factor of CO_2 and fuel sulphur content FSC (ppm M) are known, the ratio of S-atoms and CO_2-molecules in one gram fuel burnt is

$$\frac{FSC \cdot N_A}{M_S} \div \frac{EF_{CO_2} \cdot N_A}{M_{CO_2}} = \frac{FSC}{EF_{CO_2}} \cdot \frac{M_{CO_2}}{M_S} \qquad (3)$$

where N_A is the Avogadro's constant, M_{CO_2} and M_S are the mole masses of CO_2 and S. If all sulphur in the fuel is assumed to have been oxidized to SO_2, Eq. (3) approximately equals to the ratio of the measured SO_2 and CO_2 concentrations integrated under the peaks over the background concentrations. Therefore, FSC in % can be calculated by

the following equation

$$\text{FSC(\%)} = \frac{\Delta SO_2(\text{ppb}) \cdot 10^{-3}}{\Delta CO_2(\text{ppm})} \cdot \frac{M_S}{M_{CO_2}} \cdot EF_{CO_2} \cdot 100 \approx \frac{\Delta SO_2(\text{ppb})}{\Delta CO_2(\text{ppm})} \cdot 0.23 \qquad (4)$$

Based on the measured carbon mass percent of the fuels (Cooper et al., 2005), a similar equation was derived in a slightly different way by Alföldy et al. (2012).

3 Results and discussion

3.1 General overview of the harbour measurements

As an example, Fig. 4 illustrates a typical time series of particle number concentration and gaseous species in the Katajanokka terminal harbour (site 2, Fig. 1) in the morning on 8 September 2011, and near the Turku harbour (site 4, Fig. 1) in the evening on 9 August 2010.

Some interesting features can be observed. First, the approaching or leaving ships are easily distinguished from the background. Of course, catching the plume by Sniffer is very sensitive to the meteorological conditions, especially to the wind speed, direction and buoyance forces. In the Helsinki case three ships E, D, and A (Table 1) arrived the harbour at 09:40, 09:47, and 10:22 (LT), respectively; the last one left the harhour at 11:37. The peak concentrations were observed simultaneously by particles and gases. In Turku three ships G, I, and K (Table 1) first arrived the harbour passing Sniffer at 18:58, 19:30 and 19:34, respectively. Later in the evening they left the harbour in the same order and again passed Sniffer at 21:06, 21:11 and 21:15. Sniffer was first standing at site 4 (Fig. 1) but because only weak gaseous peaks were monitored, Sniffer was started at 20:00 and driven to site 2 (Fig. 1). Sniffer's own exhaust caused the small peaks in particle concentration at around 20:00. At the new site the background CO_2 concentration was somewhat higher than in the first site. Typically, the peak particle concentrations varied in the range of $10^4 - 10^6\,\text{cm}^{-3}$ when

Full Screen / Esc

Printer-friendly Version

Interactive Discussion

the ships passed Sniffer at 200–800 m distance; the maximum values were 1.5×10^6 and 1.6×10^5 cm^{-3} in Helsinki and Turku, respectively. The highest SO_2 concentrations measured during the campaigns were 168 ppb in Helsinki and 38 ppb in Turku.

Second, discharging of the passenger cars and trucks from the ship and loading into the ship occurred in Helsinki harbour at 10:33–11:18 leading to an increase in particles as well as NO_x and CO_2 concentrations whereas no peak appeared in the SO_2 concentration. The smallest nucleation mode particles (< 30 nm) dominate vehicles' exhaust emissions whereas for ships the particles larger than 30 nm are more abundant.

Third, the local background concentration in Helsinki was higher than in Turku. More detailed comparison of the background particle characters can be seen in Table 2 and Fig. 5. The average background concentrations were calculated by taking into account the lowest 5 % of the measured values of each measurement periods. The average values were then classified according to the location (Helsinki–Turku), to the season (winter–summer), and to the daytime (morning–evening). Systematically, at each site the concentrations were higher in winter compared to summer. When the wind blew from the sea (south), the average number concentration was around 10^4 cm^{-3} or even somewhat lower, and variation was rather small. However, sites 1, 4 and 5 in Turku and sites 3 and 4 in Helsinki occasionally suffer from the north-easterly wind which carries pollutants from the city center and in Turku additionally from the harbour. In these cases, the standard deviations are much higher as well.

In winter the nucleation mode is much stronger than in summer whereas the differences observed in the accumulation mode were not so significant (Fig. 5). The reason might be the lower ambient temperature which brings down the saturation ratio of the condensing vapours and thus favours nucleation as well (e.g. Pirjola et al., 2006). Additionally, the height of the mixing layer varies between winter and summer influencing the dilution of the pollutants. The concentrations are higher in the morning due to the busy morning traffic, energy production and smaller vertical mixing than in the afternoon. This kind of behaviour has been found in many vehicle studies as well (e.g. Molnár et al., 2002; Wehner et al., 2002; Virtanen et al., 2006; Pirjola et al., 2012).

3.2   Size distributions of the ship particles

Figure 6 illustrates the time series of particle number size distributions for the same measurement periods as in Fig. 4. The ship peaks take around 3 min, and can easily be distinguished from the background. Particle number and volume size distributions were plotted for four selected ships (D, E, G and I, Table 1) using different after-treatment systems (Fig. 7). For each of these ships, 7–16 successful size distributions were measured. The GPS data from the ships and our own distance measurements by the laser rangefinder showed that along the narrow shipping channel near Turku all ships operated with the constant speed of around 8.4 knots and most likely with the constant engine load. The plots show the averaged normalised size distributions, i.e. for each ship the background size distribution was subtracted from the measured size distribution, then the result was divided by the excess CO_2 concentration to remove the effect of dilution, after that the average size distribution for an individual ship along with standard deviation was calculated. This was done for the peak maximum size distribution as well as for the 50 % and 75 % of the integrated peak. Because no large variation was observed, we present here only the size distributions for the peak maximum values. Two modes were fitted, and the modal parameters (number or volume concentration of the mode divided by the excess CO_2 concentration in the units $cm^{-3} ppm^{-1}$ or $\mu m^3 cm^{-3} ppm^{-1}$, geometric mean diameter Dg in µm, and standard deviation σ) for the Aitken (or the nucleation mode if present) and the accumulation (or soot) modes are given in Table 3.

When considering the number size distributions, for all ships the Aitken modes were dominating and peaking at around 20–30 nm. The accumulation modes were typically peaking at 80–100 nm. In winter, the ships requiring water for the after-treatment systems (HAM and DWI) had clearly higher particle number and volume emissions than the others. As well the emitted particles were larger. The smallest particulate emissions were observed from the ship equipped with the SCR system. In summer, the differences between the ships were not significant with an exception of the DWI ship.

When considering the volume size distributions the accumulation mode was dominant and the Aitken mode particles can hardly be distinguished. The accumulation modes were peaking at 400–500 nm for the HAM and DWI ships, and at around 200 nm for the others. Similar results have been reported in the literature. For example, Moldanova et al. (2009) studied a ship diesel engine on board, and found that in the hot exhaust the mass size distribution showed two main modes: one in the accumulation mode at the diameter around 0.5 μm and the other in the coarse mode at 7 μm. Additionally, Fridell et al. (2008) found a third peak in the diameter range 100–200 nm in the hot exhaust. Isakson et al. (2000) reported that when the ship plume was emitted about 600 m from the instruments the dominant mode of the number size distribution was in the diameter range below 40 nm, and a weaker mode in the range of 70–100 nm. The airborne measurements by Petzold et al. (2008) showed that although the ship plume ages two modes were peaking at 14 nm and at 90–100 nm, measured in dry conditions.

In regard to all ships, the average total number concentration increases as an increase in SO_2 concentration (Fig. 8) indicating that at least a part of the nucleation mode particles might be formed by H_2SO_4-H_2O nucleation. This is in an agreement with Petzold et al. (2008) who concluded that the smallest particles (< 30 nm) were composed predominantly of sulphuric acid water clusters while the large combustion particle mode contains most of the non-volatile black carbon, organic carbon and ash. Also Lack et al. (2009) suggested that the reason for the nucleation mode particles is very fast formation of small sulphuric acid particles that subsequently grow by condensation and coagulation. Furthermore, they found that emissions of sulphate and organic matter linearly correlate with fuel sulphur content while emissions of black carbon are heavily dependent on engine type.

3.3 Volatility properties of the ship particles

Volatility properties of particles emitted from the ships on the way to the Turku harbour in 2011 were investigated by using a thermodenuder (TD) installed into the Sniffer prior to the ELPI (with the additional stage). Before the TD, the other ELPI simultaneously

measured the plume in the ambient temperature. The TD was heated to 265 °C, when most of the volatile species are expected to be evaporated. The particle losses in the thermodenuder were corrected and the background concentrations were subtracted. There were five ships operating to the harbour, but due to the meteorological conditions during the campaign, we were able to observe 12 successful peaks for only two of the ships, ships K and I in Table 1.

As an example, Fig. 9 illustrates the averaged number and volume size distributions for ship K, based on the peak values of the particles. Also shown in Fig. 9 are the size distributions for the non-volatile particles measured after the TD treatment. The error bars describe standard deviations. The size distributions for all other analysed ships showed rather similar behavior. As seen from Fig. 9a, the number size distribution of the non-volatile particles was bimodal: the nucleation mode ($N_{tot} \sim 2.3 \times 10^4 \, cm^{-3}$) was peaking at 12 nm or smaller and the accumulation ($N_{tot} \sim 5.8 \times 10^3 \, cm^{-3}$) mode at 49 nm. Note that the existence of even smaller particles than 7 nm (ELPI's detection limit) and thus smaller modal diameter than 12 nm cannot be ruled out. Jonsson et al. (2011) reported the nucleation mode diameter for the non-volatile particles at the range of 10.1–16.5 nm. Without the TD treatment the particles were larger; the Aitken mode was peaking at around 37 nm ($N_{tot} \sim 2.5 \times 10^4 \, cm^{-3}$), and the accumulation ($N_{tot} \sim 1.5 \times 10^3 \, cm^{-3}$) mode at 93 nm. Three lognormal modes peaking at 86 nm, 256 nm and 1.8 μm were fitted for the non-volatile volume size distribution whereas for all particles two modes were fitted peaking at 206 nm and 5.7 μm.

The non-volatile fraction of the particles was calculated in the range of 35–74 % by number and 29–33 % by volume. Petzold et al. (2007) used the DMPS (Differential Mobility Particle Sizer) measuring the particles > 13 nm and reported 34 ± 3 % by number and 29 ± 3 % by mass; on the other hand, Jonsson et al. (2011) reported the values between 26–66 % by number by using the EEPS (Engine Exhaust Particle Sizer) for the particle sizes 5.6–560 nm.

Title Page

Abstract | Introduction

Conclusions | References

Tables | Figures

|◄ | ►|

◄ | ►

Back | Close

Full Screen / Esc

Printer-friendly Version

Interactive Discussion

Full Screen / Esc

Printer-friendly Version

Interactive Discussion

3.4 Emission factors

For comparison the emission parameters were calculated from the peak concentration values and from the integrated surface area. Since the results were very close to each other, we present here the results based on the peak values. As an example, Fig. 10 presents the emission ratios according to Eq. (1) for NO, NO_x, SO_2, N_{tot}, and $PM_{2.5}$ for ship G (Table 1). The correlation coefficient is typically close to 0.90, and even the smallest value found for the total number concentration is 0.84. A possible explanation for this is that besides dilution, aerosol dynamics might have some effect on particle number concentration, whereas CO_2 concentration depends only on dilution. On the other hand, many authors have reported for car exhaust particles that dilution dominates and covers coagulation and condensation processes unless mixing is inefficient (see review paper by Kumar et al., 2011). Furthermore, during dilution NO_x is inert but NO is able to oxidize with ozone to form NO_2. This might cause some uncertainty to EF_{NO}, even though the time for the ship plume to transport from the source to the measurement site was in maximum 3–5 min. The calculated emission factors for ship G are $EF_{NO} \sim 13 \pm 1\,g\,(kg\,fuel)^{-1}$, $EF_{NO_x} \sim 26 \pm 2\,g\,(kg\,fuel)^{-1}$, $EF_{SO_2} \sim 5.4 \pm 0.7\,g\,(kg\,fuel)^{-1}$, $EF_{N_{tot}} \sim (1.38 \pm 0.2) \times 10^{16}$ particles $(kg\,fuel)^{-1}$, and $EF_{PM_{2.5}} \sim 2.81 \pm 0.30\,g\,(kg\,fuel)^{-1}$. Table 4 gives the average emission factors for all individual ships converted to NTP conditions. In Table 4 the ships are ordered according to the after-treatment systems. The ships equipped with the SCRs efficiently reduced the NO_x emissions, and the ships utilising water in the after-treatment systems had high $PM_{2.5}$ emissions. On the other hand, their SO_2 emissions were smallest. Should remember that the emission factors vary from ship to ship and from moment to moment since they depend on many factors such as fuel, lubricant oil, after-treatment system, ship's speed, engine load, age of the ship etc. The values presented in the literature are in the range of 2.9–6.2 and 22–109 $g\,(kg\,fuel)^{-1}$ for SO_2 and NO_x, respectively, $(0.4 - 6.2) \times 10^{16}\,(kg\,fuel)^{-1}$ for N_{tot}, and $0.5 - 3.4\,g\,(kg\,fuel)^{-1}$ for $PM_{2.5}$ (Kumar et al., 2011 and references therein).

3.5 Fuel sulphur content

An averaged fuel sulphur content FSC (in %) was estimated for each ship studied in this work (Table 5). We assumed that the individual ships used the similar fuel every time. Based on the clear SO_2 and CO_2 peaks (Fig. 4), around 5–20 successful cases were found for each ship and the averaged FSCs were calculated. It should be noted that the measured fuel sulphur content is a weighted average of the main engine and auxiliary engine sulphur emissions. If both main and auxiliary engines use fuel with identical fuel sulphur content, the measured value can be thought as direct indication of the fuel sulphur content used onboard the vessel. In the cases where main and auxiliary engines use fuels with different sulphur content, the sulphur levels will be a combination of these contributions roughly equivalent to the ratio of main engine and auxiliary engine power used at the time of the measurement. As seen from Table 5, the FSCs for all ships are less than 1 % which was set as a limit in Baltic Sea on 1 July 2010. However, none of them was below 0.1 % which is the new directive by EU (European Union, 2012) and come into effect on 1 January 2015.

4 Conclusions

Particle and gaseous emissions from the ship diesel engines with different after-treatment systems were measured by the mobile laboratory in two different environments: inside the harbour areas in Helsinki and along the narrow shipping channel near Turku, Finland. The particle number and volume size distributions as well as the volatility properties of the particles were investigated. Based on the measurements, the emission parameters and fuel sulphur contents for the 11 individual ROPAX ships were determined.

The results showed that the highest particle concentrations were 1.5×10^6 and 1.6×10^5 cm^{-3} in Helsinki and Turku, respectively, and the particle number size distribution had two modes: the dominating mode was peaking at 20–30 nm and the accumulation

Title Page

Abstract | Introduction

Conclusions | References

Tables | Figures

|◄ | ►|

◄ | ►

Back | Close

Full Screen / Esc

Printer-friendly Version

Interactive Discussion

mode at 80–100 nm. The majority of the particle mass was volatile since after heating the sample to 265 °C, the particle volume of the studied ship decreased by around 70 %. Simultaneously the modal diameters of the number size distribution shifted to 12 nm and 49 nm.

The emission factors for NO_x varied in the range of 25–100 g (kg fuel)$^{-1}$, for SO_2 in the range of 2.5–17 g (kg fuel)$^{-1}$, for particle number between (0.32–2.26) × 10^{16} (kg fuel)$^{-1}$, and for $PM_{2.5}$ 1.0–4.9 g (kg fuel)$^{-1}$. The ships equipped with SCR had lowest NO_x emissions whereas the ships with DWI and HAM had lowest SO_2 emissions but highest particulate emissions. For all ships the averages FSCs were less than 1 % but none of those was below 0.1 % which will be the new EU directive from 1 January 2015. This sets big challenges for developing better fuels and after-treatment systems in close future.

The contribution from shipping particulate emissions globally is the same order as the contribution from road traffic (Eyring et al., 2005). However, the shipping particulate emissions are only regulated through the sulphur level requirements and poor estimates are available for nanoparticle exposure. Particle size distribution measurements are also needed to improve the quantification of indirect climatic effects of particles and SO_2. Furthermore, this work might have relevance to city planning and locating harbours appropriately.

References

Agrawal, H., Welch, W. A., Miller, J. W., and Cocker, D. R.: Emission measurements form a crude oil tankder at sea, Environ. Sci. Technol., 42, 7098–7103, 2008.

Alföldy, B., Balzani Lööv, J., Lagler, F., Mellqvist, J., Berg, N., Beecken, J., Weststrate, H., Duyzer, J., Bencs, L., Horemans, B., Cavalli, F., Putaud, J.-P., Janssens-Maenhout, G., Pintér Csordás, A., Van Grieken, R., Borowiak, A., and Hjorth, J.: Measurements of air pollution emission factors for marine transportation, Atmos. Meas. Tech. Discuss., 5, 8925–8967, doi:10.5194/amtd-5-8925-2012, 2012.

Arnold, F., Pirjola, L., Aufmhoff, H., Schuck, T., Lähde, T., and Hämeri, K.: First gaseous sulphuric acid detection in automobile exhaust: implications for volatile nano-particle formation and health risk, Atmos. Environ., 40, 7097–7105, 2006.

Ault, A. P., Moore, M. J., Furutani, H., and Prather, K. A.: Impact of emissions from the Los Angeles part region on San Diego air quality during regional transport events, Environ. Sci. Technol., 43, 3500–3506, 2009.

Corbett, J. J., Winebrake, J. J., Green, E. H., Kasibhatla, P., Eyring, V., and Lauer, A.: Mortality from ship emissions: a global assessment, Environ. Sci. Technol., 41, 8512–8518, 2007.

European Union: DIRECTIVE 2012/33/EU, available at: http://eur-lex.europa.eu/LexUriServ/LexUriServ.do?uri=OJ:L:2012:327:0001:0013:EN:PDF (last access: 31 July 2013), 2012.

Eyring, V., Köhler, H. W., van Aardenne, J., and Lauer, A.: Emissions from international shipping: 1. The last 50 years, J. Geophys. Res., 110, D17305, doi:10.1029/2004JD005619, 2005.

Fridell, E., Steen, E., and Peterson, K.: Primary particles in ship emission, Atmos. Environ., 42, 1160–1168, 2008.

Fuglesvedt, J., Berntsen, T., Eyring, V., Isaksen, I., Lee, D. S., and Sausen, R.: Shipping emissions: from cooling to warming of climate- and reducing impacts on health, Environ. Sci. Technol., 43, 9057–9062, 2009.

Healy, R. M., O'Connor, I. P., Hellebust, S., Allanic, A., Sodeau, J. R., and Wenger, J. C.: Characterisation of single particles from in-port ship emissions, Atmos. Environ., 43, 6408–6414, 2009.

IMO: International Maritime Organization: regulations for the prevention of air pollution from ships and NO_x technical code, Annex VI of the MARPOL convention 73/78 London, 1998.

Title Page

Abstract	Introduction
Conclusions	References
Tables	Figures

Back | Close

Full Screen / Esc

Printer-friendly Version

Interactive Discussion

Isakson, J., Persson, T. A., and Lindgren, E. S.: Identification and assessment of ship emissions and their effects in the harbour of Göteborg, Sweden, Atmos. Environ., 35, 3659–3666, 2001.

Jalkanen, J.-P., Johansson, L., Kukkonen, J., Brink, A., Kalli, J., and Stipa, T.: Extension of an assessment model of ship traffic exhaust emissions for particulate matter and carbon monoxide, Atmos. Chem. Phys., 12, 2641–2659, doi:10.5194/acp-12-2641-2012, 2012.

Jonsson, Å. M., Westerlund, J., and Hallquist, M.: Size-resolved particle emission factors for individual ships, Geophys. Res. Lett., 38, L13809, doi:10.1029/2011GL047672, 2011.

Kasper, A., Aufdenblatten, S., Forss, A., Mohr, M., and Burtscher, H.: Particulate emissions from a low-speed marine diesel engine, Aerosol Sci. Tech., 41, 24–32, 2007.

Keskinen, J., Pietarinen, K., and Lehtimäki, M.: Electrical low pressure impactor., J. Aerosol Sci., 23, 353–360, 1992.

Kumar, P., Ketzel. M., Vardoulakis, S., Pirjola, L., and Bitter, R.: Dynamics and dispersion modelling of nanoparticles from road traffic in the urban atmospheric environment – a review, J. Aerosol Sci., 42, 580–603, 2011.

Kumar, P., Pirjola, L., Ketzel, M., and Harrison, R. M.: Nanoparticle emissions from 11 non-vehicle exhaust sources – a review, Atmos. Environ., 67, 252–277, 2013.

Lack, D. A., Corbett, J. J., Onasch, T., Lerner, B., Massoli, P., Quinn, P. K., Bates, T. S., Covert, D. S., Coffman, D., Sierau, B., Herndon, S., Allan, J., Baynard, T., and Lovejoy, E. A.: Particulate emission from commercial shipping: chemical, physical and optical properties, J. Geophys. Res., 114, D00F04, doi:10.1029/2008JD011300, 2009.

Lyyränen, J., Jokiniemi, J., Kauppinen, E. I., and Joutsensaari, J.: Aerosol characterisation in medium-speed diesel engines operating with heavy fuel oils, J. Aerosol Sci., 30, 771–784, 1999.

Malkki, M., Lounasheimo, J., Niemi, J., Myllynen, M, and Loukkola, K.: Air quality in the Helsinki Metropolitan Area in 2010, HSY publications 3/2011, 2011.

Malkki, M., Matilainen, L., Kousa, A., Niemi, J., and Loukkola, K.: Air quality in the Helsinki Metropolitan Area in 2011, HSY publications 9/2012, 2012.

Marjamäki, M., Ntziachristos, L., Virtanen, A., Ristimäki, J., Keskinen, J., Moisio, M., Palonen, M., and Lappi, M.: Electrical filter stage for the ELPI, Society of Automotive Engineers (SAE) Technical Paper 2002–01–0055, 2002.

Molnár, P., Janhäll, S., and Hallquist, M.: Roadside measurements of fine and ultrafine particles at a major road north of Gothenberg, Atmos. Environ.,36, 4115–4123, 2002.

Mobile measurements of ship emissions

L. Pirjola et al.

Title Page

Abstract	Introduction
Conclusions	References
Tables	Figures

Back | Close

Full Screen / Esc

Printer-friendly Version

Interactive Discussion

Moldanova, J., Fridell, E., Popovicheva, O., Demirdjian, B., Tishkova, V., Faccinetto, A., and Focsa, C.: Characterisation of particulate matter and gaseous emissions from a large ship diesel engine, Atmos. Environ., 43, 2632–2641, 2009.

Morawska, L., He, C., Hitchins, J., Mengersen, K., and Gilbert, D.: Characteristics of particle number and mass concentrations in residential houses in Brisbane, Australia, Atmos. Environ., 37, 4195–4203, 2003.

Murphy, S. M., Agrawal, H., Sorooshian, A., Padroì, L. T., Gates, H., Hersey, S., Welch, W. A., Jung, H., Miller, J. W., Cocker, D. R., Nenes, A., Jonsson, H. H., Flagan, R. C., and Seinfeld, J. H.: Comprehensive simultaneous shipboard and airborne characterization of exhaust from a modern container ship at sea, Environ. Sci. Technol., 43, 4626–4640, 2009.

Petzold, A., Hasselbach, J., Lauer, P., Baumann, R., Franke, K., Gurk, C., Schlager, H., and Weingartner, E.: Experimental studies on particle emissions from cruising ship, their characteristic properties, transformation and atmospheric lifetime in the marine boundary layer, Atmos. Chem. Phys., 8, 2387–2403, doi:10.5194/acp-8-2387-2008, 2008.

Pirjola, L., Parviainen, H., Hussein, T., Valli, A., Hämeri, K., Aalto, P., Virtanen, A., Keskinen, J., Pakkanen, T., Mäkelä, T., and Hillamo, R.: "Sniffer" – a novel tool for chasing vehicles and measuring traffic pollutants, Atmos. Environ., 38, 3625–3635, 2004.

Pirjola, L., Paasonen, P., Pfeiffer, D., Hussein, T., Hämeri, K., Koskentalo, T., Virtanen, A., Rönkkö, T., Keskinen, J., Pakkanen, T. A., and Hillamo, R. E.: Dispersion of particles and trace gases nearby a city highway: mobile laboratory measurements in Finland, Atmos. Environ., 40, 867–879, 2006.

Pirjola, L., Lähde, T., Niemi, J. V., Kousa, A., Rönkkö, T., Karjalainen, P., Keskinen, J. Frey, A., and Hillamo, R.: Spatial and temporal characterization of traffic emission in urban microenvironments with a mobile laboratory, Atmos. Environ., 63, 156–167, 2012.

Rönkkö, T., Arffman, A., Karjalainen, P., Lähde, T., Heikkilä, J., Pirjola, L., Rothe, D., and Keskinen, J.: Diesel exhaust nanoparticle volatility studies by a new thermodenuder with low solid nanoparticle losses, Abstracts in the 15th ETH-Conference on Combustion Generated Nanoparticles, 26–29 June 2011, Zürich, Switzerland, 2011.

Saxe, H. and Larsen, T.: Air pollution from ships in three Danish ports, Atmos. Environ., 38, 4057–4067, 2004.

Schlager, H., Baumann, R., Lichtenstern, M., Petzold, A., Arnold, F., Speidel, M, Gurk, C., and Fisher, H.: Aircraft-based trace gas measurements in a primary European ship corridor.

Mobile measurements of ship emissions

L. Pirjola et al.

Title Page

Abstract | Introduction

Conclusions | References

Tables | Figures

|◄ | ►|

◄ | ►

Back | Close

Full Screen / Esc

Printer-friendly Version

Interactive Discussion

Proceedings of the International Conference on Transport, Atmosphere and Climate, Oxford, June 2006, TAC Extended Abstracts, 2007.

Sinha, P., Hobbs, P. V., Yokelson, R. J., Christian, T. J., Kirchstetter, T. W., and Bruintjes, R.: Emissions of trace gases and particles from two ships in the southern Atlantic Ocean, Atmos. Environ., 37, 2139–2148, 2003.

Turku: Turun kaupunkiseudun ilmanlaaturaportti vuonna 2011; http://www.turku.fi/Public/default.aspx?nodeid=12085 (last access: 31 July 2013), 2011 (in Finnish with English abstract).

Virtanen, A., Rönkkö, T., Kannosto, J., Ristimäki, J., Mäkelä, J. M., Keskinen, J., Pakkanen, T., Hillamo, R., Pirjola, L., and Hämeri, K.: Winter and summer time size distributions and densities of traffic-related aerosol particles at a busy highway in Helsinki, Atmos. Chem. Phys., 6, 2411–2421, doi:10.5194/acp-6-2411-2006, 2006.

Wehner, B., Birmili, W., Gnauk, T., and Wiedensohler, A.: Particle number size distribution in a street canyon and their transformation into the urban air background: measurements and a simple model study, Atmos. Environ., 36, 2215–2223, 2002.

Wierzbicka, A.: What are the characteristics of airborne particles that we are exposed to?, Doctoral thesis, Lund University, Department of Design Sciences, 2008.

Yli-Ojanperä, J., Kannosto, J., Marjamäki, M., and Keskinen, J.: Improving the nanoparticle resolution of the ELPI, Aerosol. Air. Qual. Res., 10, 360–366, 2010.

Title Page

Abstract | Introduction

Conclusions | References

Tables | Figures

|◄ | ►|

◄ | ►

Back | Close

Full Screen / Esc

Printer-friendly Version

Interactive Discussion

Table 1. Technology parameters of the ships. SRC = Selective Catalytic Reduction, HAM = Humid Air Motor, DWI = Direct Water Injection, CC = Catalytic Converter.

Ship	Ship type	Engine manu-facturer	Engine Model	Main en-gines	After-treatment system	Max. power (MW)	Year
A	ROPAX	Wärtsilä	46 F	4	SCR	40.0	2008
B	ROPAX	Wärtsilä	16V32	4	SCR	32.0	2008
C	ROPAX	Wärtsilä	12V46C	4	NONE	50.4	2008
D	ROPAX	Wärtsilä	12PC2-6V-400	4	HAM	23.0	1985
E	ROPAX	Wärtsilä	9R46	4	DWI	32.6	1991
F	ROPAX	Wärtsilä	9R46	4	DWI	32.6	1990
G	ROPAX	MAN	6L58/64	4	SCR	31.8	1993
H	ROPAX	Wärtsilä	16V32	4	SCR	26.2	2006
I	ROPAX	Pielstick	12PC2-6V-400	4	NONE	23.8	1989
J	ROPAX	Pielstick	12PC2-6V-400	4	NONE	23.8	1988
K	ROPAX	MaK	8M453 AK	4	NONE	7.4	1972

Title Page

Abstract · Introduction

Conclusions · References

Tables · Figures

|◄ · ►|

◄ · ►

Back · Close

Full Screen / Esc

Printer-friendly Version

Interactive Discussion

Table 2. Average background number concentrations with standard deviations during the harbour measurements.

Helsinki				Turku			
Site	Wind direc- tion	N_{tot} $(10^3\,cm^{-3})$ winter	N_{tot} $(10^3\,cm^{-3})$ summer	Site	Wind direc- tion	N_{tot} $(10^3\,cm^{-3})$ winter	N_{tot} $(10^3\,cm^{-3})$ summer
1, 2	S	8.8 ± 1.4	7.8 ± 2.3	1, 5	SW, NE	22.3 ± 4.3	11.9 ± 1.4
3	E, NE	32.6 ± 5.3	12.4 ± 9.4	2	W, E	11.3 ± 2.1	8.8 ± 1.3
4	E, NE	51.1 ± 4.9	7.1 ± 4.3	3, 7	S, SW	9.8 ± 1.6	6.8 ± 1.3
7	S	–	7.2 ± 2.4	4	S, SW, NE	21.0 ± 3.7	16.2 ± 3.2
				8	S, SW	–	6.3 ± 1.0

Table 3. Modal parameters (number concentration N, geometric mean diameter Dg, standard deviation σ) for the ships mentioned in Fig. 5. Different after-treatment systems (ATS) are given in the first column.

ATS	winter Aitken mode			winter accumulation mode			summer Aitken mode			summer accumulation mode		
	N (cm^{-3} ppm^{-1})	Dg (nm)	σ	N (cm^{-3} ppm^{-1})	Dg (nm)	σ	N (cm^{-3} ppm^{-1})	Dg (nm)	σ	N (cm^{-3} ppm^{-1})	Dg (nm)	σ
NONE	2591	29	1.56	704	75	1.39	8358	33	1.92	–	–	–
HAM	10 535	31	1.85	1327	100	2.06	6869	26	1.77	2070	82	1.64
DWI	7333	33	1.73	2246	85	1.85	3902	26	1.77	1524	75	1.81
SCR	1934	19	1.77	776	77	1.60	5491	23	1.64	3100	82	1.64

Discussion Paper | Discussion Paper | Discussion Paper | Discussion Paper | Discussion Paper

AMTD

6, 7149–7184, 2013

Mobile measurements of ship emissions

L. Pirjola et al.

Title Page

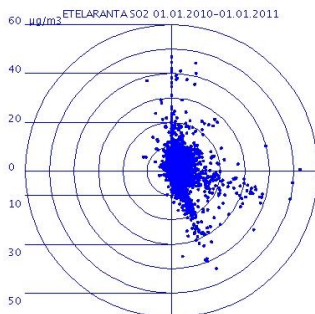Abstract | Introduction

Conclusions | References

Tables | Figures

|◄ | ►|

◄ | ►

Back | Close

Full Screen / Esc

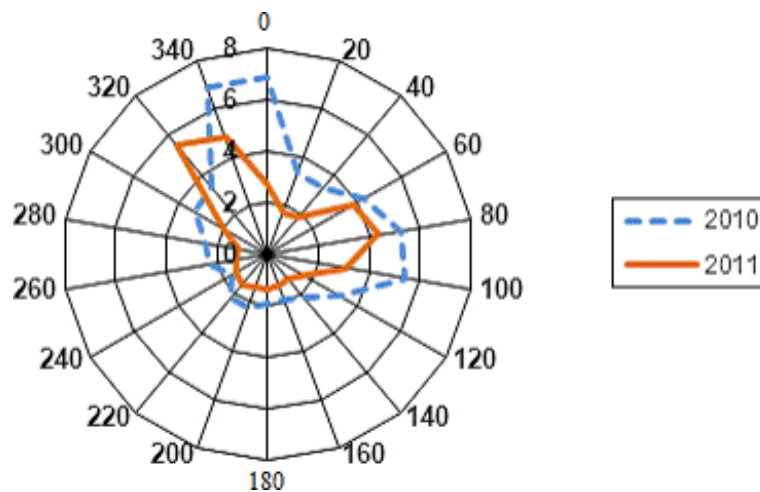Printer-friendly Version

Interactive Discussion

Table 4. Emission factors in NTP conditions ($p = 1.013 \times 10^5$ Pa, $T = 293.15$ K).

ATS	EF_{NO} $(g\,(kg\,fuel)^{-1})$	EF_{NO_x} $(g\,(kg\,fuel)^{-1})$	EF_{SO_2} $(g\,(kg\,fuel)^{-1})$	$EF_{N_{tot}}$ $(10^{16}\,(kg\,fuel)^{-1})$	$EF_{PM_{2.5}}$ $(g\,(kg\,fuel)^{-1})$
NONE	42 ± 6	65 ± 10	9.8 ± 1.0	1.25 ± 0.17	2.54 ± 0.40
NONE	72 ± 14	86 ± 13	4.6 ± 0.6	1.86 ± 0.27	2.24 ± 0.29
NONE	53 ± 9	86 ± 15	8.7 ± 1.9	1.45 ± 0.30	1.58 ± 0.82
NONE	55 ± 6	76 ± 6	5.7 ± 0.6	1.72 ± 0.22	4.90 ± 0.48
HAM	34 ± 8	56 ± 12	3.5 ± 0.1	0.39 ± 0.19	2.87 ± 2.05
DWI	57 ± 13	100 ± 23	2.5 ± 1.0	*	3.26 ± 1.58
DWI	47 ± 29	*	*	1.34 ± 0.62	1.05 ± 0.85
SCR	49 ± 6	79 ± 9	9.9 ± 0.1	2.26 ± 0.83	*
SCR	29 ± 3	44 ± 4	17.0 ± 1.2	0.32 ± 0.21	1.00 ± 1.58
SCR	18 ± 1	26 ± 2	5.4 ± 0.7	1.38 ± 0.20	2.81 ± 0.30
SCR	16 ± 8	25 ± 15	6.3 ± 0.1	*	2.19 ± 0.33

* A coefficient of determination (R^2) for Emission Ratio-fit low, < 0.2.

Table 5. Estimated fuel sulphur contents along with standard deviations for all ships studied in this work.

Ship	FSC (%)
A	0.68 ± 0.26
B	0.84 ± 0.10
C	0.62 ± 0.18
D	0.41 ± 0.16
E	0.33 ± 0.10
F	0.34 ± 0.18
G	0.31 ± 0.13
H	0.38 ± 0.06
I	0.38 ± 0.15
J	0.37 ± 0.13
K	0.46 ± 0.16

Fig. 1. Measurement sites in Helsinki South Harbour (sites 1–4) and West Harbour (site 7), and along the shipping channel near Turku Harbour (sites 1–8). (©OpenStreetMap contributors, CC BY-SA, see http://www.openstreetmap.org/).

(a)

(b)
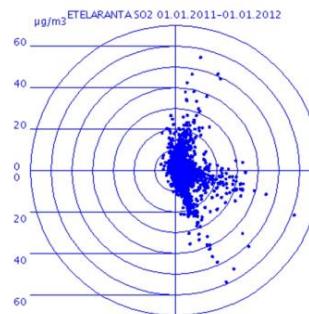
Fig. 2. Hourly SO$_2$ concentrations in μg m^{-3} in South Harbour, Helsinki, during years 2010 **(a)** (Malkki et al., 2011), and 2011 **(b)** (Malkki et al., 2012).

Title Page

Abstract | Introduction

Conclusions | References

Tables | Figures

|◄ | ►|

◄ | ►

Back | Close

Full Screen / Esc

Printer-friendly Version

Interactive Discussion

Fig. 3. Hourly SO_2 concentration in $\mu g\,m^{-3}$ in Ruissalo, Turku, during years 2010 and 2011 (Turku, 2011).
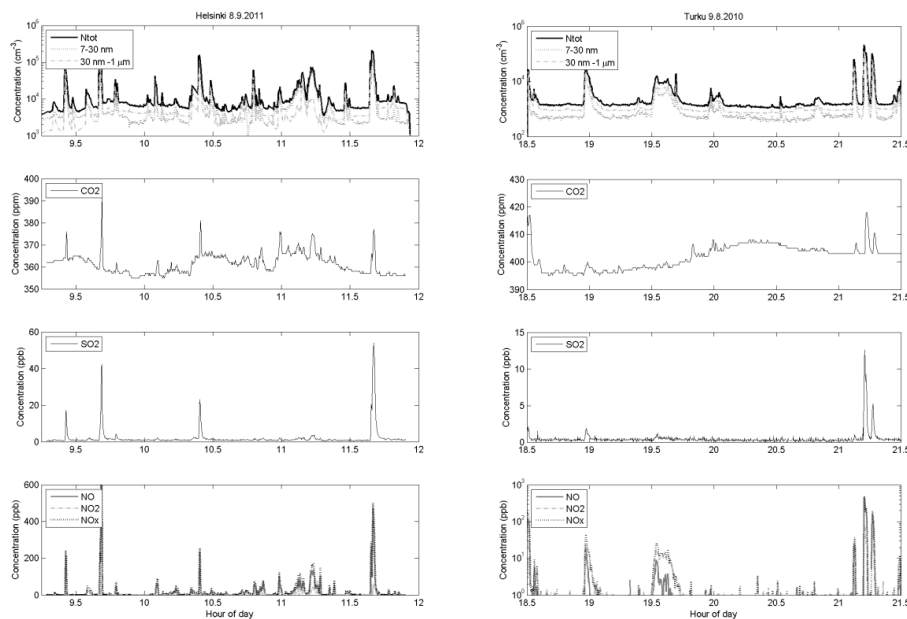
Fig. 4. Shown are time series of particle number concentration, gaseous CO_2, SO_2, NO, NO_2 and NO_x in Helsinki on 8 September 2011 (left side) and in Turku on 9 August 2010 (right side). Besides total number concentration, concentrations of particles smaller than 30 nm and in the range of 30–1000 nm are shown as well.

(a)

(b)
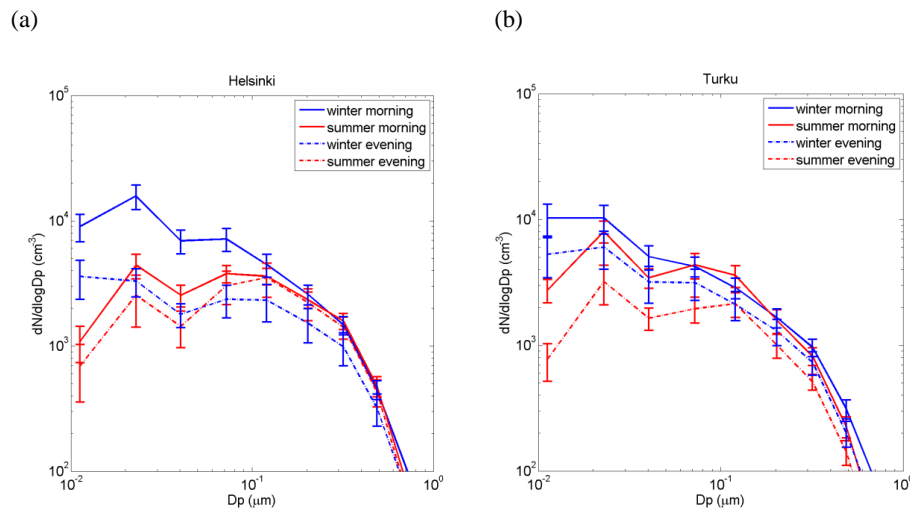
Fig. 5. Average number size distributions of background particles during winter and summer in Helsinki **(a)**, and in Turku **(b)**. Also shown are the curves for morning and evening measurements. Error bars refer to the standard deviations.

(a)

(b)

Fig. 6. Time series of particle number size distributions dN/d log Dp (cm^{-3}) in Helsinki **(a)** and Turku **(b)** for the same time periods as in Fig. 4. Y-axis refers to particle diameter Dp in m. Color bar shows the concentration dN/d log Dp (cm^{-3}). The ships are marked by arrows and denominated according to Table 1.
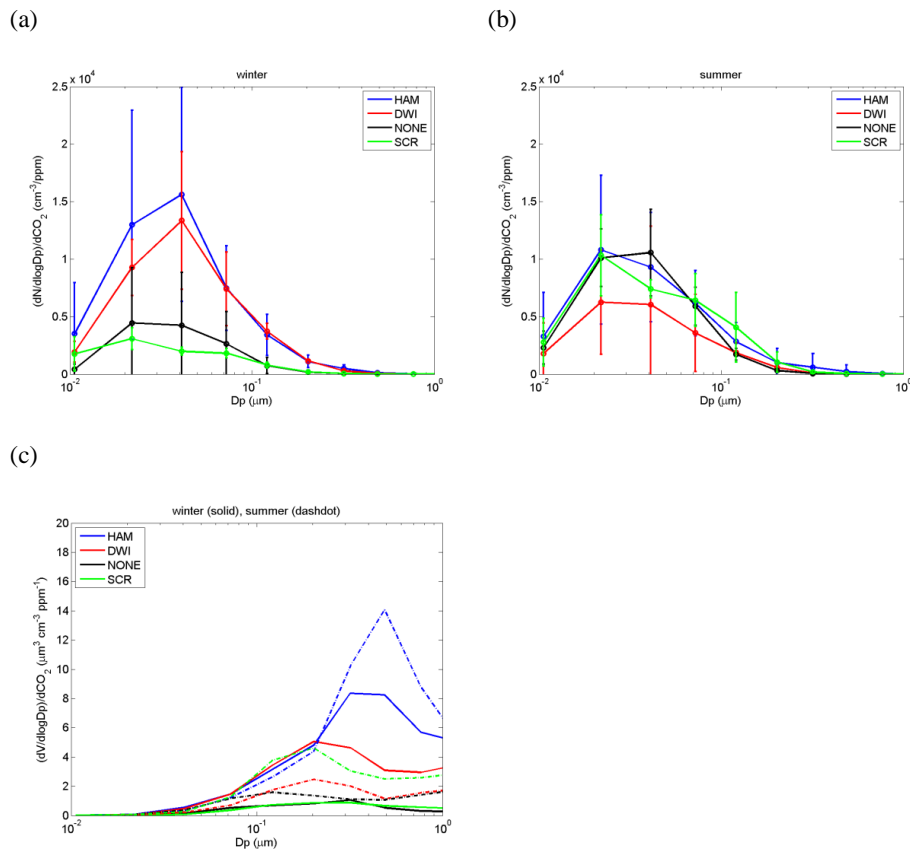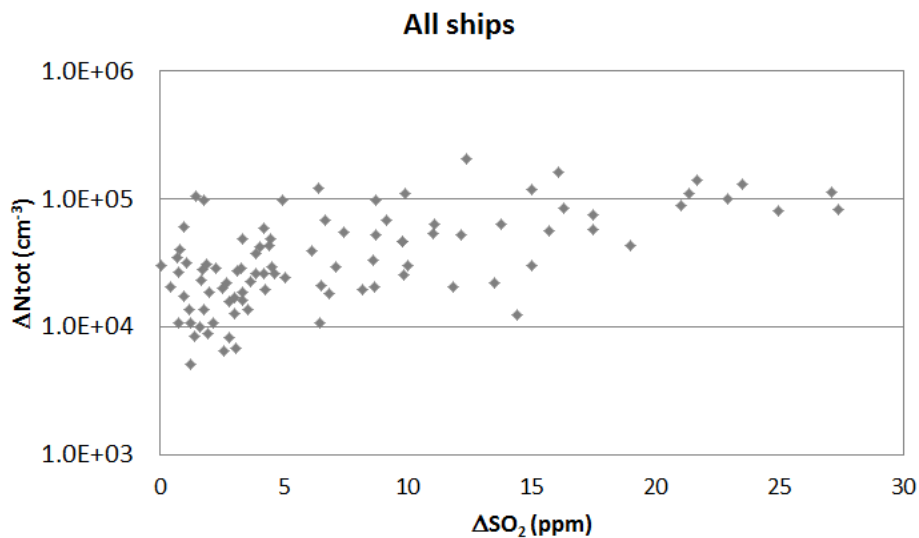
Fig. 7. Normalised number size distributions for winter **(a)** and summer **(b)** for the ships using different after-treatment systems. The corresponding volume size distributions are presented in **(c)**. The error bars show the standard deviations.

Title Page

Abstract Introduction

Conclusions References

Tables Figures

◄ ►

◄ ►

Back Close

Full Screen / Esc

Printer-friendly Version

Interactive Discussion

Fig. 8. Correlation of particle number concentration and SO_2.

(a)

(b)
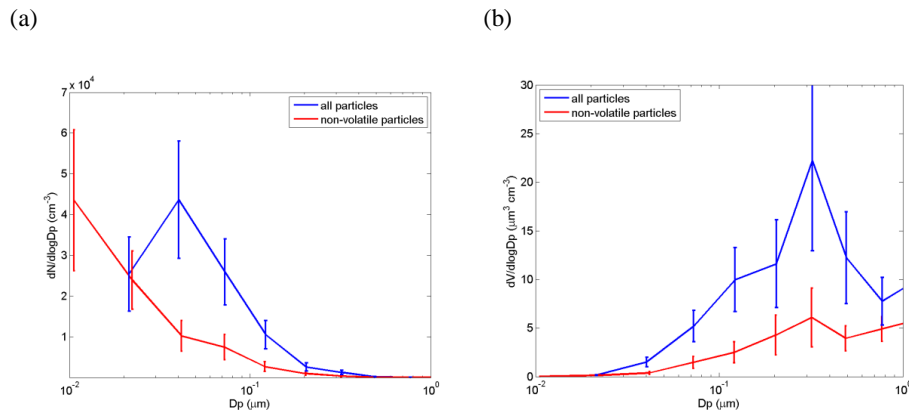
Fig. 9. Particle number **(a)** and volume **(b)** size distributions measured with the thermodenuder treatment (non-volatile particles) and without it (all particles) for ship K which had no after-treatment system. The error bars describe standard deviations.

Discussion Paper | Discussion Paper | Discussion Paper | Discussion Paper |

AMTD

6, 7149–7184, 2013

Mobile measurements of ship emissions

L. Pirjola et al.

Title Page

Abstract | Introduction

Conclusions | References

Tables | Figures

|◄ | ►|

◄ | ►

Back | Close

Full Screen / Esc

Printer-friendly Version

Interactive Discussion
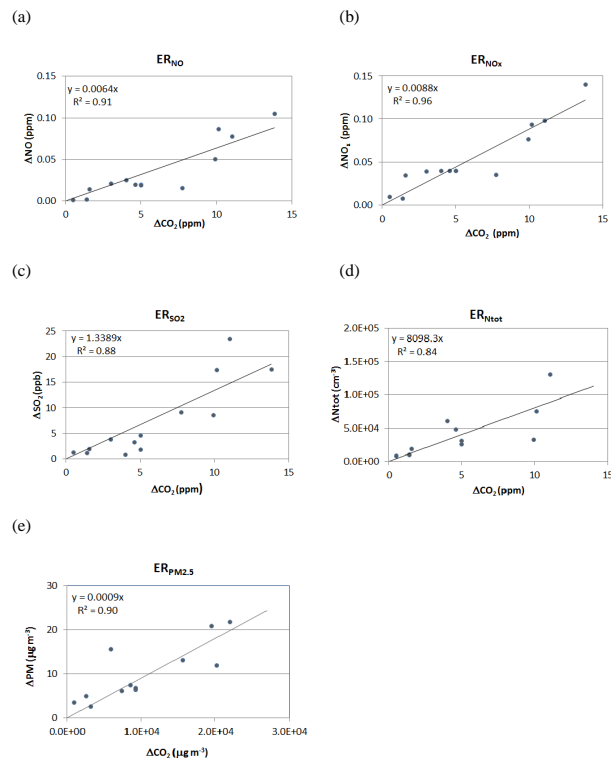
Fig. 10. Emission ratios of NO **(a)**, NO_x **(b)**, SO_2 **(c)**, N_{tot} **(d)**, and $PM_{2.5}$ **(e)** for ship G. The units are $ppm\,ppm^{-1}$, $cm^{-3}\,ppm^{-1}$ and $\mu g\,m^{-3}\,(\mu g\,m^{-3})^{-1}$ for gases, particle number and mass concentration, respectively. Also shown are the slopes and correlation coefficients.